Supplemental Information (Supplementary Methods and Supplementary Figures)

Supplementary Methods

Immunostaining

Neurons were fixed in 4% paraformaldehyde, 4% sucrose in 1x phosphate buffered saline (PBS) for 20 minutes, rinsed 2 x 5 minutes in 1x PBS and blocked in 3% bovine serum albumin, 0.15% Triton-X in 1x PBS for 30 minutes. Primary antibody diluted in blocking solution was applied to neurons for 2 hours, neurons were rinsed 3 x 5 minutes each in blocking solution, and secondary antibodies were then applied in block for 45 minutes. Neurons were again washed 3 x 8 minutes each in blocking solution, followed by a final wash in PBS before they were coverslipped. The following primary antibodies were used for this study: Chicken anti-MAP2 (1:5000; Abcam, Cambridge, MA), Guinea pig anti-VGLUT 1 (1:5000; Millipore) and Guinea pig anti-VGLUT 2 (1:1000; Millipore), mouse anti-GAD6 (1:50; Developmental Studies Hybridoma Bank, Iowa City, IA), Goat anti-GFP (1:3000; Abcam), mouse anti-Bassoon (1:1000; Abcam), mouse anti-NR1 (1:500; BD Pharmingen), mouse anti-PSD-95 (1:250; Affinity Bioreagents) and rabbit anti-DsRed to visualize mCherry (1:1000; ClonTech, Mountain View, CA). Appropriate secondary antibodies raised in donkey were used (1:1000; Jackson Immunoresearch, West Grove, PA).

For live-labeling experiments, antibodies were diluted in Opti-MEM (Invitrogen) supplemented with 0.05% sodium azide (to prevent receptor internalization) and added to living neurons for 10 minutes. Neurons were then rapidly washed 4 times in Opti-MEM and fixed. Staining then proceeded as described above. The following primary antibodies were used for live-labeling experiments: rabbit anti-GluR1 (1:10; EMD Biosciences, San Diego, CA), mouse anti-GluR2 (1:100; Millipore) rabbit anti-GFP (Invitrogen; 1:1000). mouse anti-Flag (1:1000; Sigma), and mouse anti-myc (1:1000; Covance).

Images were captured on a Leica SP2 confocal microscope (McBain Instruments, Chatsworth, CA) with a 63x oil-immersion objective at 3x zoom and were analyzed using NIH ImageJ. The number of VGLUT, GAD6, GluR1 or GluR2 positive puncta per 10 μm of dendrite was calculated after images were thresholded (cutoff at approximately 15 x background; all micrographs within an experiment were thresholded with the same

cutoff). For experiments in which MAP2 was used as a dendrite marker, all puncta within 1 μm of the dendrite were included in the data set to account for puncta on spines. All analysis was of proximal dendrites within 200 μm of the cell soma. Inhibitory neurons were identified by GAD6 positive cell bodies and were excluded from the data set. The density of neurons was monitored by MAP2 staining and all captured and analyzed neurons were plated at a standard density. All conditions were repeated in duplicate or triplicate wells within a given experiment and were repeated across several independent cultures. All image capturing and analysis was done blind to condition. The acquisition and analysis parameters were identical for all conditions within a given experiment.

Plasmids

CFP:GluR1 c-tail and CFP:GluR2 c-tail constructs were made following the description in Shi et al. 2001 (Shi et al., 2001). GluR1 and GluR2 NTD constructs were made by subcloning the first 400 amino acids of GluR1 and GluR2 into the pDisplay vector (Invitrogen). This resulted in an NTD that had an Ig κ-chain leader sequence fused to its N-terminal side and a platelet derived growth factor receptor (PDGFR) transmembrane domain fused to its c-terminal side. This allowed for trafficking of the GluR NTDs to the membrane surface and proper orientation of the NTD in the extracellular space (see Supplementary Fig. 3). For creating the GluR2 NTD deletion constructs, forward primers starting at the codon for amino acid 110 (TCCTTCATCACACCTAGCTTCCCAACA) and at the codon for amino acid 174 (CAGGTGACTGCTATCAATGTGGGGAAC) were used. The reverse primer was the same as the one used for the GluR2-NTD construct.

Live Imaging

One hour imaging experiments: Cells were grown on glass coverslips which were transferred into a custom-built holder at the time of imaging. The holder was fitted onto the stage of an Olympus Fluoview 300 upright confocal microscope (Olympus Center Valley, PA) encased in a custom-built plexiglass chamber and the cells were continuously perfused with artificial CSF (124mM NaCl, 5 mM KCl, 26 mM NaHCO3, 1.23 mM NaH2PO4, 2 mM MgCl2, 2 mM CaCl2, and 10 mM glucose) bubbled with 95% O_2 / 5% CO_2. Images were acquired with a 63x water-immersion objective at 3x zoom. After identifying an area of interest containing a Syn-GFP expressing axon, a z-stack was set that began at least 5 μm above and ended 5 μm below the plane of interest.

This ensured that Syn-GFP puncta didn't drift out of the imaging field within the z-plane. A z-stack (step interval 0.5-1.0 μm) was acquired every 10 minutes for 1 hour.

Six hour imaging experiments: Cells were plated on glass-bottom dishes (MatTek Corporation, Ashland, MA) and were imaged on an inverted Nikon fluorescent microscope (Nikon Instruments, Inc., Melville, NY) at 0, 3 and 6 hour time points. Cells were returned to the incubator between imaging time points. After the 3rd imaging point, cells were live-labeled for GluR1 or GluR2 or fixed and stained with anti-NR1 antibodies.

Simultaneous imaging of Syn-GFP puncta and mCherry-expressing dendrites: In a subset of experiments, we imaged the dynamics of Syn-GFP puncta in contact with dendrites expressing mCherry (Figs 2, 5, and 7j). We transfected a subset of neurons at 4 DIV with Syn-GFP and a separate subset of neurons at 7 DIV with mCherry +/- additional constructs to manipulate AMPA receptor surface expression (see results for details). At 12 DIV, we located sites where Syn-GFP expressing axons contacted mCherry positive dendrites and we imaged the dynamics of these contacts every 10 minutes for 1 hour. Neurons were plated at a slightly lower density (45,000/cm^2) in these experiments to minimize the presence of non-transfected dendrites in the imaging plane. For each experiment, we verified that mCherry expressing dendrites were the only dendrites in the field of view by DIC imaging. Fields of view containing non-transfected dendrites were not analyzed.

Analysis of Imaging Experiments

Z-stacks were collapsed into a maximum projection image in NIH ImageJ and were thresholded at 15 x background. Although X-Y drift was essentially nil in these experiments, all alignments were checked and corrected if necessary using the plug-in ManualAlignerC, downloaded from the ImageJ website. Z-projections for each time point were then assembled into a sequential stack and were analyzed using a custom plug-in for ImageJ written by Tom Maddock. This program parsed through each stack and identified the location of every punctum that appeared at any point during the imaging window. A circle with a 2.5 μm diameter was then placed around each punctum and the presence or absence of a punctum within that region of interest was scored for every time point within the experiment. Using the data generated by this program, we carried out two types of analysis. In the first analysis, we determined the fraction of imaged puncta that were newly added, eliminated or stable across 1 hour (Fig. 1h). Newly added

puncta appeared during imaging and persisted for at least 2 consecutive frames. Eliminated puncta were present for at least two consecutive frames before disappearing (defined as a complete loss of signal). In a second analysis, we determined a dwell time for each punctum (Fig. 1i-j). If a punctum was present in a single image frame, it was assigned a dwell time of 0 minutes. If a punctum was present in two consecutive imaging frames, but was absent in the flanking time points, it was assigned a dwell time of 10 minutes and so forth. Puncta that were present across the entire imaging period were "stable". In this analysis, we removed from the data set any puncta that were present at the start of imaging but disappeared by the last frame, as well as puncta that appeared during the imaging period and persisted through the last imaging period.

Image acquisition and analysis for all imaging experiments presented in this paper were done blind to condition. The acquisition and analysis parameters were identical for all conditions within a given experiment.

293T cell imaging assay

We cotransfected 293T cells with mCherry (for visualization) along with various combinations of plasmids (see Fig. 8). Twelve hours post-transfection, 293T cells were seeded onto 10-11 DIV neurons expressing Syn-GFP (transfected at 4 DIV). Interactions between Syn-GFP puncta and 293T cells were imaged 18-24 hours post-overlay across 1 hour. Z-stacks were acquired every 10 minutes.

Following imaging, z-stacks were maximum-projected and assembled into movies. In each case, we confirmed that Syn-GFP puncta were in direct contact with 293T cells by parsing through optical sections before creating a z-stack. Using an automated analysis program for ImageJ (described above), we determined a "stability index" for each 239T cell, defined as the fraction of stable relative to total (trafficking + stable) Syn-GFP puncta contacting that cell. This gave us a number that described the ability of the 293T cell to effectively capture and stabilize trafficking Syn-GFP puncta. Inclusion criteria for 293T cells were (1) an axon clearly contacted and crossed the 293T cell and (2) Syn-GFP puncta trafficked along this length of axon. Axons additionally were required to have both stable and trafficking puncta at some point along their length within the larger field of view.

Supplementary Figures

Figure S1. Dynamics of presynaptic inputs during synaptogenesis

(A-D) Development of excitatory presynaptic inputs in cortical cultures. Neurons were stained with antibodies against the excitatory presynaptic markers VGLUT 1& 2 (red) and the dendritic marker MAP2 (blue) at 6, 10, 14, and 18 DIV. Scale bar, 10 μm. (E) Quantification of excitatory (VGLUT positive) inputs for each neuronal age. Few excitatory inputs were seen at 6 DIV (1.6 ± 0.33 inputs/10 μm of dendrite; mean ± s.e.m.). The number increased by 10 DIV (7.8 ± 1.5) peaked at 14 DIV (14 ± 1.7), then decreased by 18 DIV (5.8 ± 0.68), suggesting that only a subset of presynaptic inputs observed at 14 DIV were stabilized. Overall p-value < 0.0001. Inter-group comparisons: *** p <0.001, ** p < 0.01, * p< 0.05. n=8-20 fields of view for each time point. (F) Representative axon segment from an 11 DIV neuron expressing Syn-GFP, imaged every 10 minutes for 1 hour. The blue arrows point to dynamic puncta.
(G) Representative axon segment from a 14 DIV neuron expressing Syn-GFP. The red arrow points to a stable Syn-GFP punctum. The yellow arrow points to a punctum that was eliminated by the 4th frame. Scale bar, 2 μm. (H) Quantification of the fraction of newly added, eliminated, and stable Syn-GFP puncta observed across synaptogenesis. Only Syn-GFP puncta that were present during at least two consecutive imaging frames were quantified to reduce the likelihood of analyzing trafficking vesicles. The fraction of stable puncta increased dramatically between 11 and 17 DIV. n=3 experiments. Total number of puncta: 546 (11 DIV), 212 (14 DIV), and 383 (18 DIV). Error bars, s.e.m. (I) Schematic of the imaging paradigm. Puncta present in a single imaging frame were assigned a dwell time of 0 minutes. Puncta present throughout the entire imaging experiment were identified as stable. (J) Quantification of dwell times at 14 DIV. Analysis revealed at least 2 separate populations of Syn-GFP puncta with distinct dynamics: a transient population (63 ± 9.9%) and a stable population (37 ± 9.8%). n=3 experiments (566 puncta, 19 fields of view). Error bars, s.e.m.

Figure S2. Localization of AMPA receptors at presynaptic sites

(A-D) Examples of AMPA receptor staining at 6, 10, 14 and 18 DIV. Surface GluR1 and GluR2 are depicted in red and green, respectively. VGLUT 1 & 2 staining is shown in blue. The merged image of all three channels is shown for each developmental age. White arrows point to examples of AMPA receptor clusters colocalized with VGLUT 1 &

2. Scale bar, 1 μm. (E) Quantification of the number of AMPA receptor (GluR1 and/or GluR2) puncta colocalized with VGLUT puncta per 10 μm of dendrite. n=8-15 fields of view for each time point. Error bars, s.e.m.

Figure S3. Syn-GFP punctum size is a good indicator of stability of presynaptic vesicles (A) Quantification of Syn-GFP size as a function of punctum dynamics. In general, the longer the dwell time, the larger the Syn-GFP punctum was. n=288 stable puncta, 189 puncta with dwell time of 0 minutes, and 78 puncta with dwell time of 10-40 minutes. Error bars, s.e.m. (B) Colocalization of bassoon and Syn-GFP as a function of Syn-GFP size. Syn-GFP puncta were separated into 3 size groups: < 0.15 μm^2, 0.15-0.9 μm^2, and > 0.9 μm^2, which corresponded with average dwell times of 0, 10-40 or > 60 minutes (see a). The fraction of Syn-GFP puncta within each group that colocalized with the presynaptic terminal marker bassoon is graphed here.
(C) Colocalization of synaptotagmin uptake staining and Syn-GFP as a function of Syn-GFP size. Syn-GFP puncta were separated into 3 size groups: < 0.15 μm^2, 0.15-0.9 μm^2, and > 0.9 μm^2, which corresponded with average dwell times of 0, 10-40 or > 60 minutes (see a). 56% of Syn-GFP puncta < 0.15 μm^2 in size colocalized with synaptotagmin uptake staining, suggesting that roughly half of puncta this size are located at active release sites. In contrast, puncta 0.15-0.9 μm^2 and > 0.9 μm^2 in size colocalized with synaptotagmin staining 96% and 92% of the time, respectively, suggesting that nearly all puncta of this size are located at sites of active neurotransmitter release.

Figure S4. DNQX blockade increases the number of excitatory presynaptic inputs (A-C) Examples of 14 DIV neurons stained with MAP2 (green). Neurons were treated from 7-14 DIV with either vehicle (DMSO, A), 20 μM DNQX (B) or 50 μM D-APV (C). The lower panels show staining of MAP2 (green) along with staining of VGLUT 1 & 2 (red). Scale bar, 5 μm. (D) Quantification of the number of excitatory (VGLUT positive) inputs per dendrite length onto vehicle (1.0 ± 0.10 VGLUT inputs), DNQX (2.1 ± 0.21 VGLUT inputs) and APV treated neurons (1.0 ± 0.13 VGLUT inputs). The number of VGLUT positive puncta per length of dendrite is normalized to control values. Overall p-value < 0.0001. Inter-group comparisons: *** p< 0.001. n=46-50 neurons for each condition. (E) Quantification of the number of surface GluR1 puncta per length of dendrite (normalized to controls). DNQX treatment led to a significant increase in surface

GluR1 puncta (2.1 ± 0.32 GluR1 puncta) in comparison to DMSO treatment (1.0 ± 0.16 GluR1 puncta) or APV treatment (1.0 ± 0.25 GluR1 puncta). Overall p-value=0.0002. Inter-group comparisons: ** p< 0.01, *** P<0.001. n=23-25 neurons for each condition. (F) Quantification of the number of surface GluR2 puncta per length of dendrite (normalized to controls). DNQX treatment led to a significant increase in surface GluR2 puncta (2.1 ± 0.19 GluR2 puncta) in comparison to DMSO treatment (1.0 ± 0.12 GluR2 puncta) or APV treatment (1.0 ± 0.14 GluR2 puncta). Overall p-value < 0.0001. Inter-group comparisons: *** p< 0.001. n=19-20 neurons for each condition.

Figure S5. Confirmation of construct expression in 293T cells

(A-C) 293T cells cotransfected with GluR1 & 2 and flag-NLG-1. Live-labeling of GluR1 & 2 (green, A) and NLG-1 (red, B) confirmed that the constructs were expressed and targeted to the membrane surface. (C) Merged image of A & B.

(D-G) 293T cells transfected with myc-GluR1 NTD (D), myc-GluR2 NTD (E), myc-GluR2NTD:Del1 (Δ109 amino acids) (F), and myc-GluR2NTD:Del2 (Δ173 amino acids) (G). Cells were live-labeled with anti-myc antibodies (red) to selectively visualize surface-expressed constructs. GluR NTDs were expressed and targeted to the membrane surface.

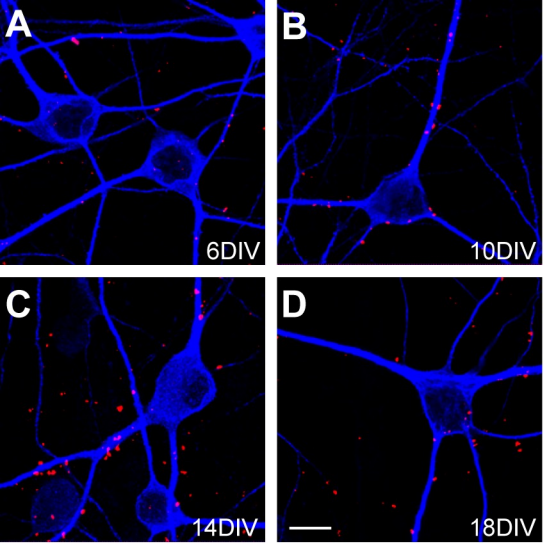
A
6DIV
B
10DIV
C
14DIV
D
18DIV

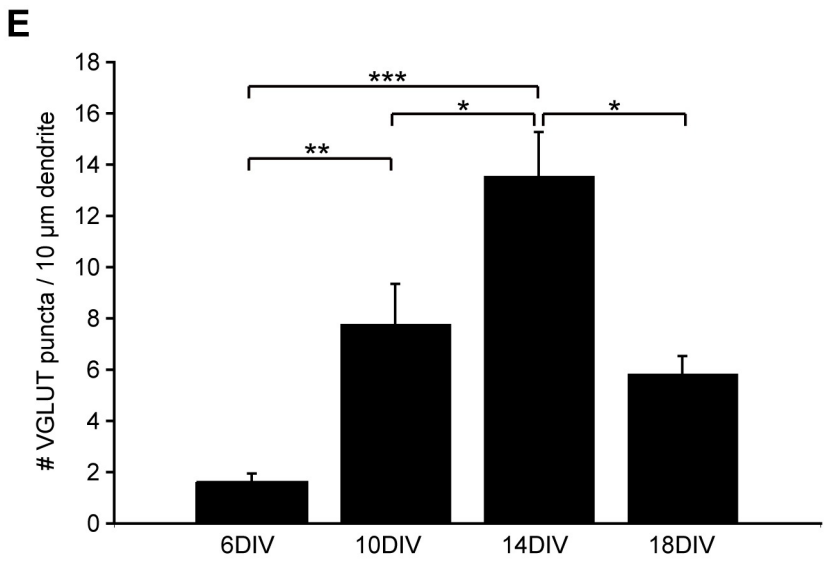
E
VGLUT puncta / 10 µm dendrite
0
2
4
6
8
10
12
14
16
18
***
*
*
**
6DIV
10DIV
14DIV
18DIV

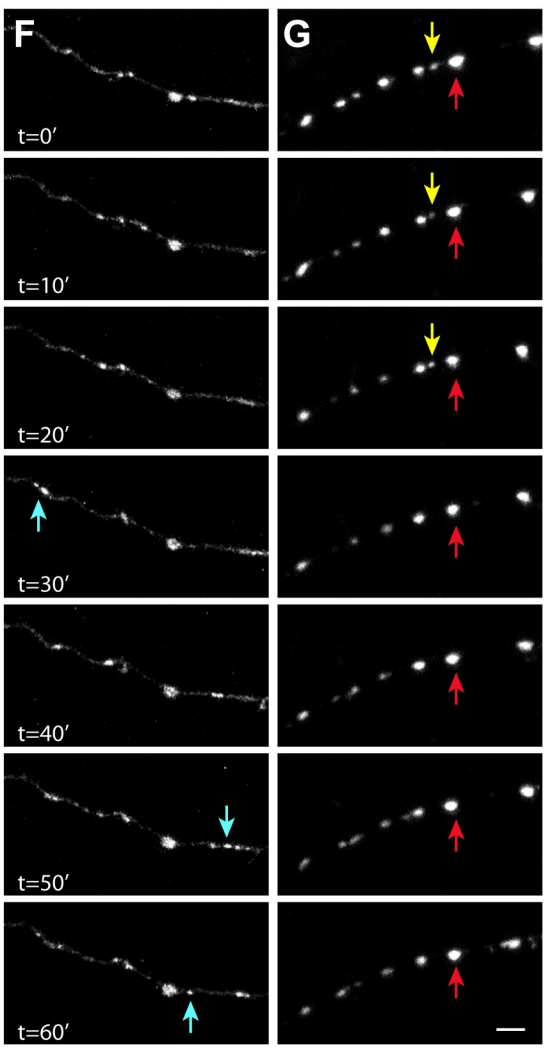
F
G
t=0′
t=10′
t=20′
t=30′
t=40′
t=50′
t=60′

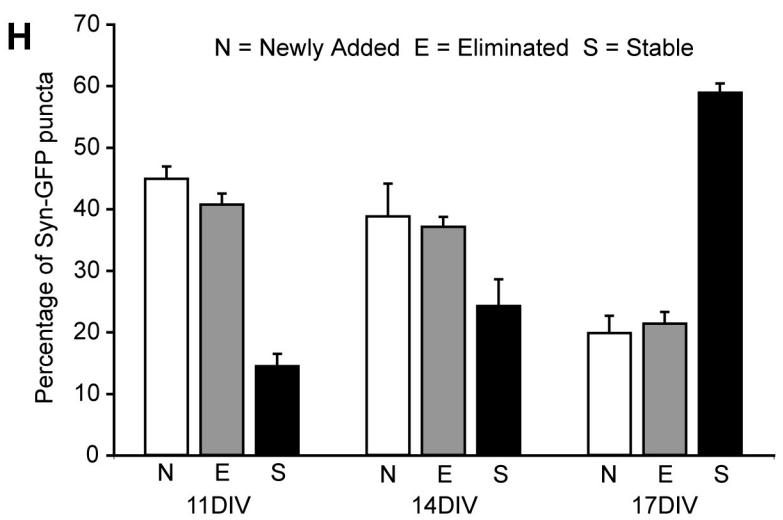
H
N = Newly Added E = Eliminated S = Stable
Percentage of Syn-GFP puncta
0
10
20
30
40
50
60
70
N E S
11DIV
N E S
14DIV
N E S
17DIV

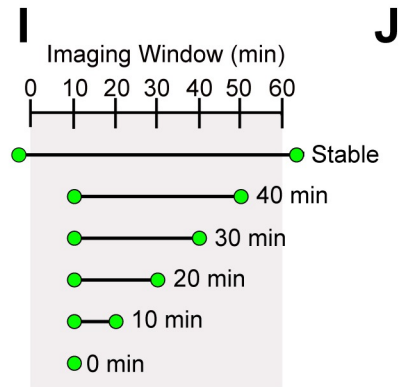
I
Imaging Window (min)
0 10 20 30 40 50 60
Stable
40 min
30 min
20 min
10 min
0 min

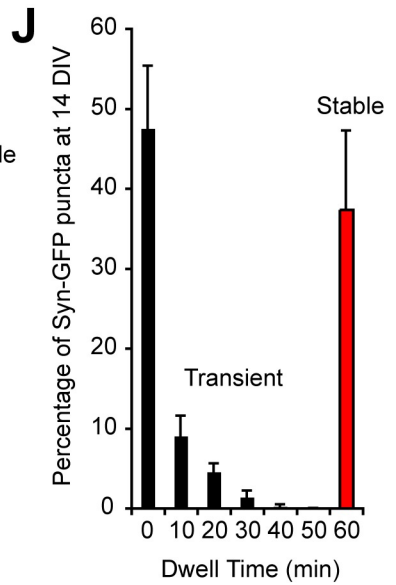
J
Percentage of Syn-GFP puncta at 14 DIV
0
10
20
30
40
50
60
Stable
Transient
0 10 20 30 40 50 60
Dwell Time (min)

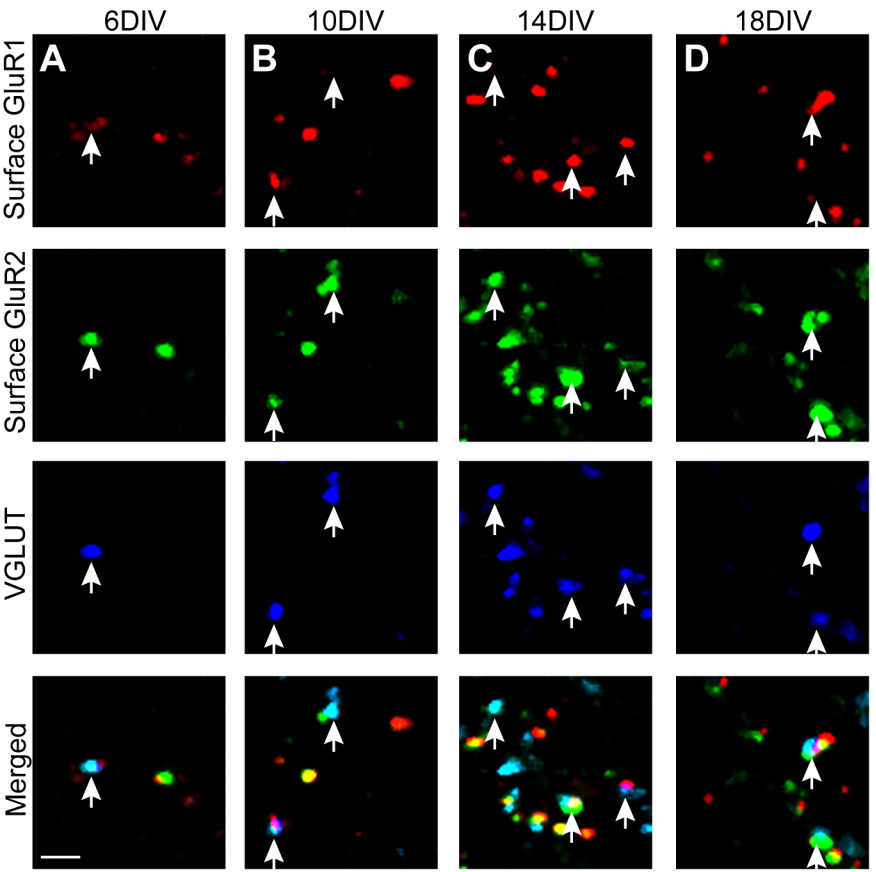
6DIV
10DIV
14DIV
18DIV
A
B
C
D
Surface GluR1
Surface GluR2
VGLUT
Merged

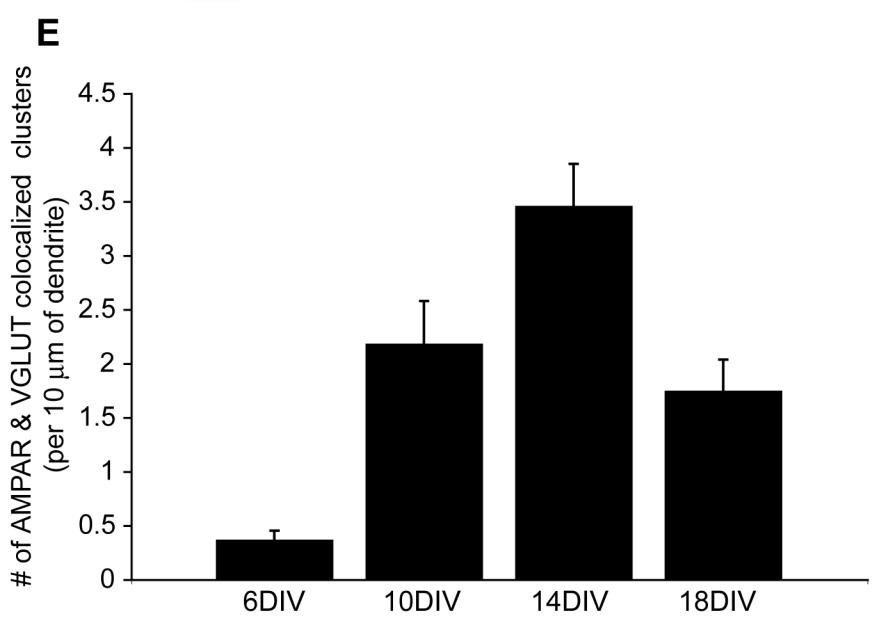
E
# of AMPAR & VGLUT colocalized clusters
(per 10 µm of dendrite)
4.5
4
3.5
3
2.5
2
1.5
1
0.5
0
6DIV
10DIV
14DIV
18DIV

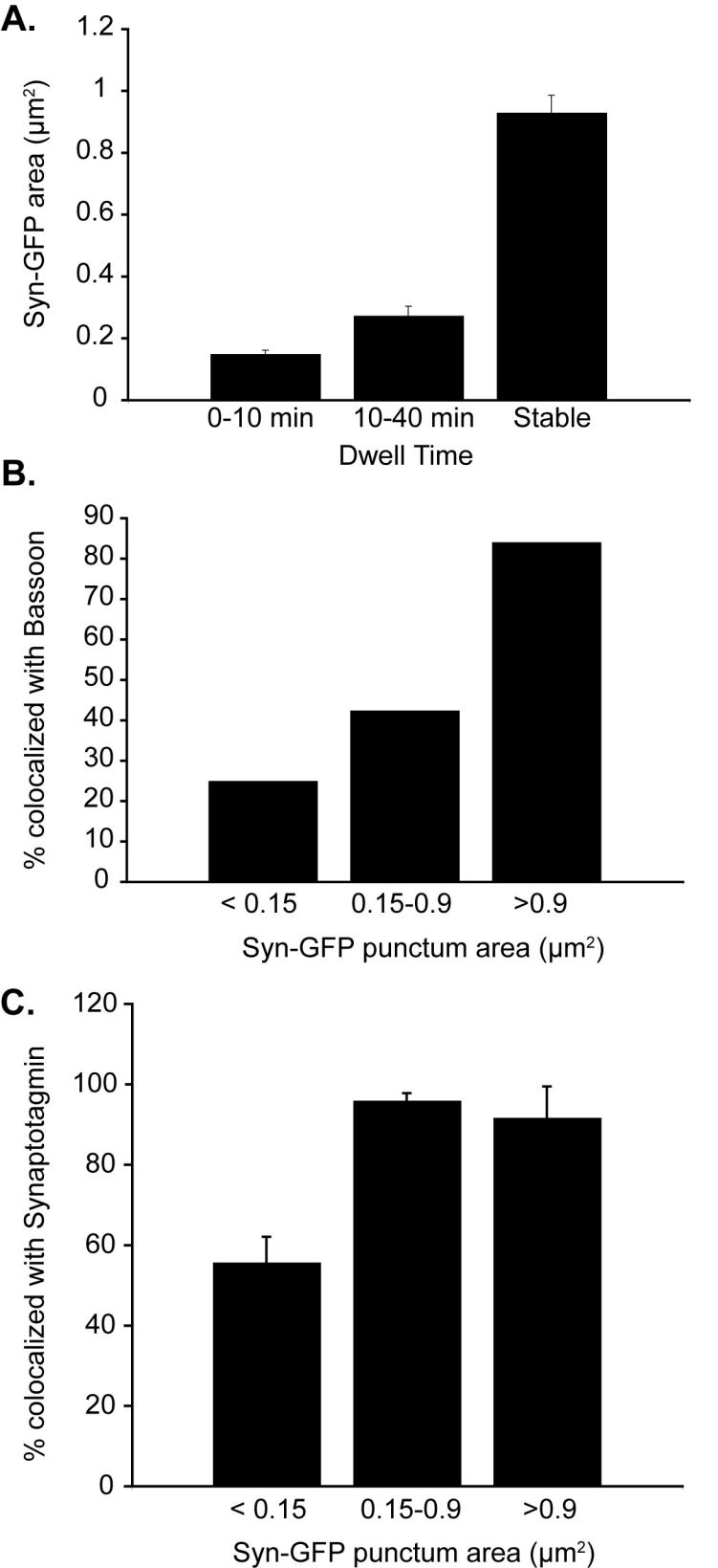
A.
Syn-GFP area (µm²)
1.2
1
0.8
0.6
0.4
0.2
0
0-10 min
10-40 min
Stable
Dwell Time
B.
% colocalized with Bassoon
90
80
70
60
50
40
30
20
10
0
< 0.15
0.15-0.9
>0.9
Syn-GFP punctum area (µm²)
C.
% colocalized with Synaptotagmin
120
100
80
60
40
20
0
< 0.15
0.15-0.9
>0.9
Syn-GFP punctum area (µm²)

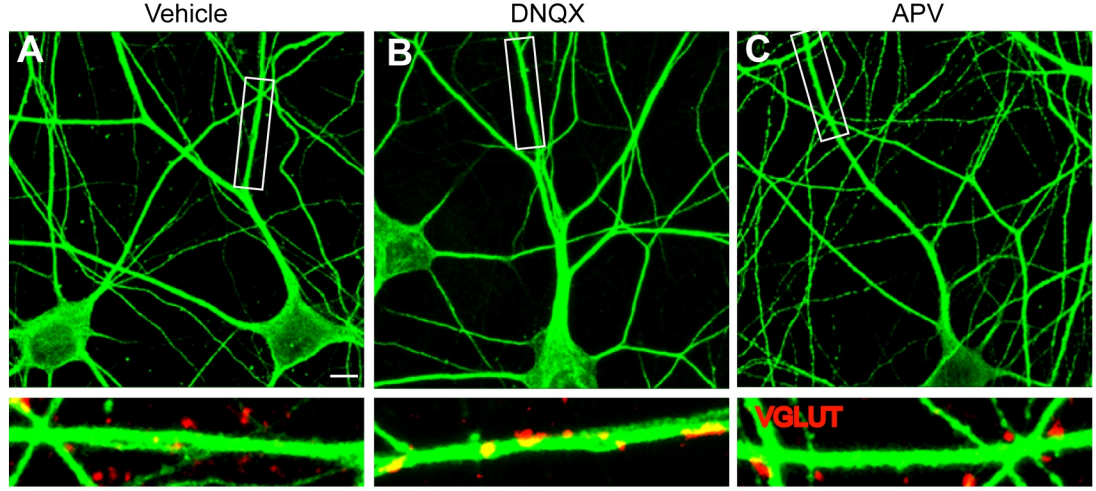
Vehicle
DNQX
APV
A
B
C
VGLUT

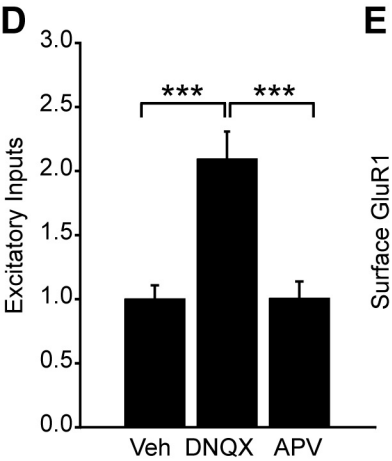
D
Excitatory Inputs
3.0
2.5
2.0
1.5
1.0
0.5
0.0
***
***
Veh
DNQX
APV

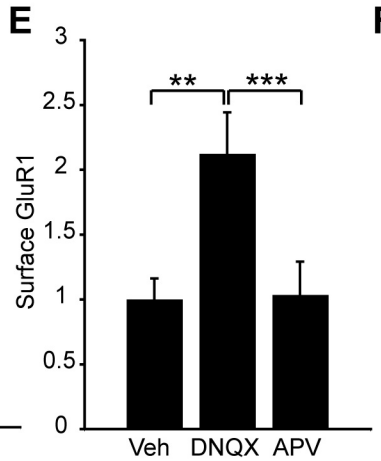
E
Surface GluR1
3
2.5
2
1.5
1
0.5
0
**
***
Veh
DNQX
APV

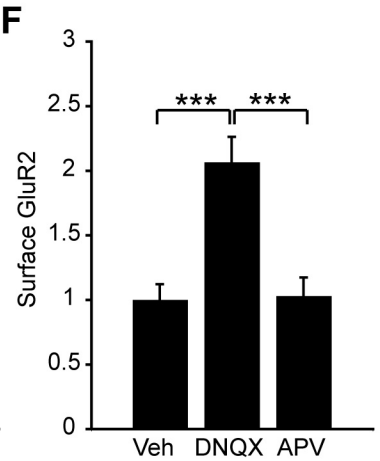
F
Surface GluR2
3
2.5
2
1.5
1
0.5
0
***
***
Veh
DNQX
APV

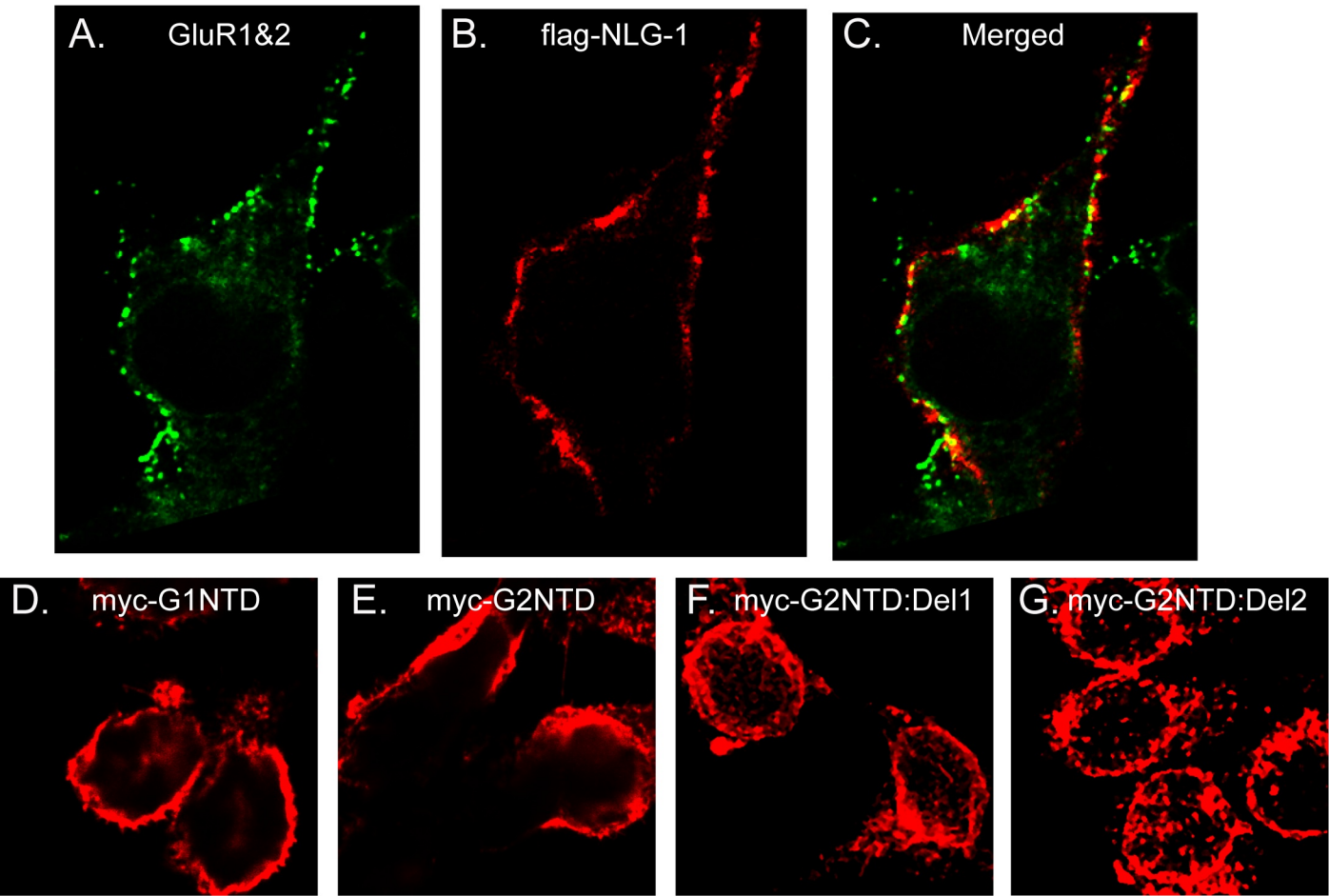
A. GluR1&2
B. flag-NLG-1
C. Merged
D. myc-G1NTD
E. myc-G2NTD
F. myc-G2NTD:Del1
G. myc-G2NTD:Del2